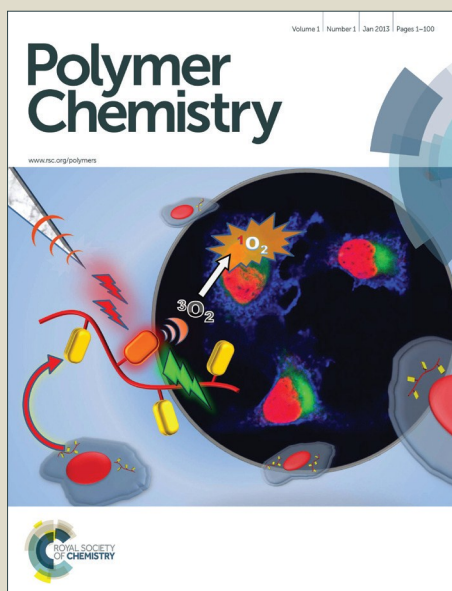


Polymer Chemistry

Accepted Manuscript



This is an *Accepted Manuscript*, which has been through the Royal Society of Chemistry peer review process and has been accepted for publication.

Accepted Manuscripts are published online shortly after acceptance, before technical editing, formatting and proof reading. Using this free service, authors can make their results available to the community, in citable form, before we publish the edited article. We will replace this *Accepted Manuscript* with the edited and formatted *Advance Article* as soon as it is available.

You can find more information about *Accepted Manuscripts* in the [Information for Authors](#).

Please note that technical editing may introduce minor changes to the text and/or graphics, which may alter content. The journal's standard [Terms & Conditions](#) and the [Ethical guidelines](#) still apply. In no event shall the Royal Society of Chemistry be held responsible for any errors or omissions in this *Accepted Manuscript* or any consequences arising from the use of any information it contains.

Novel Naphthalimide-amine Based Photoinitiators Operating under Violet and Blue LEDs and Usable for Various Polymerization Reactions and Synthesis of Hydrogels.

Nicolas Zivic,^b Jing Zhang,^a David Bardelang,^b Frédéric Dumur,^b Pu Xiao,^{*,a} Thomas Jet,^{a,c} Davy-Louis Versace,^c Céline Dietlin,^a Fabrice Morlet-Savary,^a Bernadette Graff,^a Jean Pierre Fouassier,¹ Didier Gimes,^b and Jacques Lalevée^{*,a}

^a Institut de Science des Matériaux de Mulhouse IS2M, UMR CNRS 7361, UHA, 15, rue Jean Starcky, 68057 Mulhouse Cedex, France.

^b Aix-Marseille Université, CNRS, Institut de Chimie Radicalaire ICR, UMR 7273, 13397 Marseille, France.

^c Institut de Chimie et des Matériaux Paris-Est - UMR 7182, Université Paris-Est Créteil (UPEC), Equipe "Systèmes Polymères Complexes", 2-8 rue Henri Dunant, 94320 Thiais, France.

Corresponding Authors: jacques.lalevee@uha.fr; pu.xiao@uha.fr

Abstract:

A series of naphthalimide derivatives containing tertiary amine groups (DNNDs) have been prepared. Some of these derivatives (*e.g.* DNND3, DNND4 and DNND5) exhibit interesting shifted absorption so that they can be utilized as versatile photoinitiators upon exposure to various violet and blue LEDs (385, 405, 455 and 470 nm). They are particularly efficient for the cationic photopolymerization of an epoxide and the free radical photopolymerization of an acrylate. The thiol-ene photopolymerization as well as the synthesis of interpenetrating polymer networks (of epoxide/acrylate blend) IPNs is feasible. Remarkably, the production of hydrogels can also be easily achieved using a DNND derivative after inclusion in a cyclodextrin cavity. The photochemical mechanisms are comprehensively investigated by steady state photolysis, Electron Spin Resonance (ESR), fluorescence, electrochemistry and laser flash photolysis and discussed in detail.

Keywords: naphthalimide derivatives, photoinitiator, light emitting diode (LED), violet LED, blue LED.

¹ Formerly, ENSCMu-UHA, 3 rue Alfred Werner, 68093 Mulhouse Cedex, Fr

Introduction:

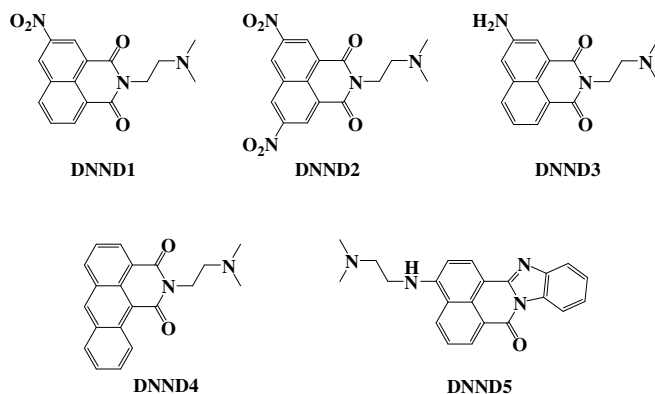
As known, the photopolymerization techniques are convenient methods to produce polymeric materials (*e.g.* coatings, inks, adhesives, dental materials, biomaterials, nanomaterials etc.).¹⁻⁴ They require the presence of reactive species *e.g.* radicals, cation radicals or cations [that are generated from a photoinitiator (PI) or a photoinitiating system (PIS)] being able to initiate the polymerization reaction during the exposure to a light source.³⁻⁵ As illustrated in recent books, chapters, reviews and papers (see relevant references *e.g.* in refs.^{1, 6-25}), extensive work has been devoted to the design of PIs and PISs for the free radical polymerization (FRP) of acrylates, the cationic polymerization (CP) of epoxides, the concomitant FRP/CP of acrylates/epoxides, the thiol-ene polymerization, the polymerization of water-borne systems, the two-photon polymerization or the controlled polymerizations.

Mercury-based UV lamps have been largely used in industrial applications. However, it is necessary and urgent to find suitable alternatives to the Hg lamps due to environmental concerns. In addition, the Governing Council of the United Nations Environment Program has also been encouraging the reduction of mercury-containing devices (Minamata Convention on Mercury). Recently, the light-emitting diode (LED) technology for photopolymerization reactions (violet LED *e.g.* 385 nm, 395 nm and 405 nm, blue LED *e.g.* 455 and 470 nm) has emerged and gained a widespread acceptance due to a lot of advantages including faster on/off switching, lower heat generation (no IR light), lower energy consumption, longer lamp lifetime, no ozone release, and improved robustness, to name but a few.^{26, 27} The design of specifically adapted high-performance PISs is one of the most significant factors for successful further developments of LED based devices in the photopolymerization area. Recent examples of such works can be encountered *e.g.* in refs.^{18, 28, 29}. A particularly huge challenge is the development of highly versatile PISs being able to efficiently initiate upon

ecofriendly LEDs all the photopolymerization modes: i) the free radical polymerization, ii) the cationic polymerization, iii) the thiol/ene, iv) the synthesis of interpenetrating polymer network (IPN) and v) the polymerization in water for hydrogel synthesis. In our previous studies, various naphthalimide or isoquinolinone derivatives³⁰⁻³⁵ have been developed as photoinitiators and the derivatives with suitable substituents exhibited excellent photoinitiating ability of polymerization. It is still interesting to further investigate the substituent effect of this kind of derivatives on their photochemical properties and expand the knowledge in the field of photoinitiators.

In the present paper, we focus our efforts on the introduction of different substituents onto the *N*-[2-(dimethylamino)ethyl]-1,8-naphthalimide skeleton. Four compounds containing nitro (DNND1 and DNND2) or amino (DNND3) substituents or anthracene (DNND4) are prepared [two of them are anti-cancer drugs referred as amonafide (DNND3) and azonafide (DNND4)³⁶]. The fifth compound is a little different as it belongs to the isoquinolinone series (DNND5). These five chemicals have been incorporated as PIs into photoinitiating systems where they are combined with an iodonium salt (Iod) or a chlorotriazine (R-Cl) and optionally *N*-vinylcarbazole (NVK) or an amine (MDEA or EDB). The FRP of a triacrylate, the CP of a diepoxide, the thiol-ene polymerization of a trithiol/divinylether blend, the synthesis of an interpenetrating polymer network from an epoxy/acrylate blend as well as the formation of hydrogels (using the PI encapsulated into a cyclodextrin cavity) upon exposure to various violet and blue LEDs (emission wavelengths from 385 nm to 470 nm) is investigated by Real-Time Fourier Transform Infrared spectroscopy (RT-FTIR). Moreover, a water-soluble DNND/cyclodextrin complex is used for the production of hydrogels. The absorption properties are studied by molecular orbital calculations and the photochemical mechanisms involved in the formation of the reactive species have been investigated by steady state

photolysis, fluorescence, cyclic voltammetry, electron spin resonance spin trapping and laser flash photolysis techniques.



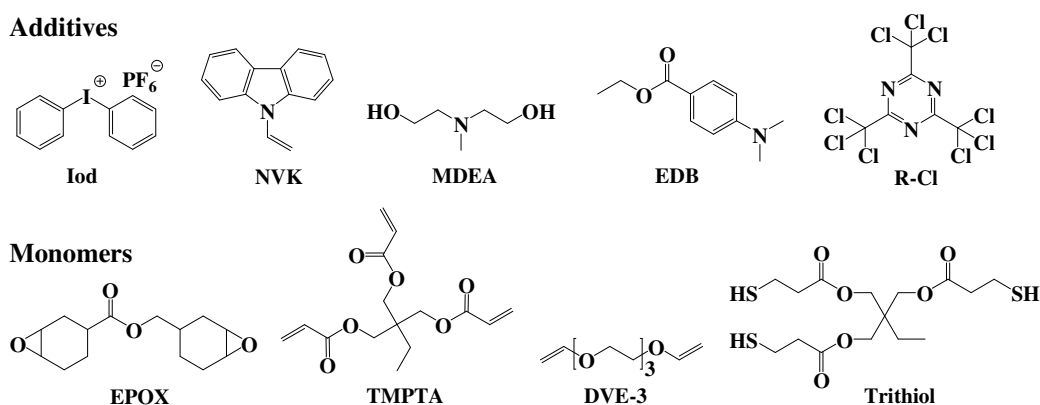
Scheme 1. Chemical structures of the DNNDs investigated as photoinitiators in this study.

Experimental

Materials

The investigated photoinitiators - *N*-[2-(dimethylamino)ethyl]-1,8-naphthalimide derivatives (DNND1 and DNND2), azonafide (DNND3), azonafide (DNND4), and isoquinolinone derivative (DNND5) - are shown in Scheme 1, while other chemical compounds are depicted in Scheme 2. DNND1 – DNND5 were synthesized according to the procedures presented in detail in the supporting information (SI). In DNND5, isomers also existed in the product as presented in the SI. Diphenyliodonium hexafluorophosphate (Iod), *N*-vinylcarbazole (NVK), methyl diethanolamine (MDEA), 2,4,6-*tris*(trichloromethyl)-1,3,5-triazine (R-Cl), camphorquinone (CQ), tri(ethylene glycol) divinyl ether (DVE-3), trimethylolpropane *tris*(3-mercaptopropionate) (Trithiol), and the other reagents and solvents were purchased from Sigma-Aldrich or Alfa Aesar and used as received without further purification. Bisacylphosphine oxide (Irgacure 819 or BAPO) was obtained from BASF. Trimethylolpropane triacrylate (TMPTA) and (3,4-epoxycyclohexane)methyl 3,4-

epoxycyclohexylcarboxylate (EPOX) were obtained from Allnex and used as benchmark monomers for radical and cationic photopolymerizations. Hydroxyethylacrylate (HEA) and hydroxyethylmethacrylate (HEMA) from Sigma-Aldrich were used as reference monomers for polymerization in water. Sulfobutylether- β -cyclodextrin (SBE- β -CD) was a generous gift of Clemens Glaubitz (Institute for Biophysical Chemistry, Goethe University Frankfurt, Germany).



Scheme 2. Chemical structures of the additives and the monomers.

Irradiation Sources

Different light sources were used for the irradiation of photocurable samples: LEDs centered at 365 nm (M365L2 – ThorLabs; $\sim 18 \text{ mW cm}^{-2}$), at 385 nm (M385L2 – ThorLabs; $\sim 27 \text{ mW cm}^{-2}$), at 405 nm (M405L2 – ThorLabs; $\sim 110 \text{ mW cm}^{-2}$), at 455 nm (M455L3 – ThorLabs; $\sim 80 \text{ mW cm}^{-2}$), at 470 nm (M470L3 – ThorLabs; $\sim 70 \text{ mW cm}^{-2}$), and a halogen lamp (Fiber-Lite, DC-950; polychromatic light; incident light intensity: $\sim 12 \text{ mW cm}^{-2}$ in the 370-800 nm range). The emission spectra of the irradiation sources are given in the SI (Figure S1-S6).

Computational Procedure

Molecular orbital calculations were carried out with the Gaussian 03 package. The electronic absorption spectra for the DNND derivatives were calculated from the time-dependent density functional theory at B3LYP/6-31G* level on the relaxed geometries calculated at UB3LYP/6-31G* level; the molecular orbitals involved in these transitions were extracted.^{37, 38} The geometries were frequency checked.

Photopolymerization Experiments

For photopolymerization experiments, the conditions are given in the Figure captions. The photosensitive formulations (25 μm thick) were deposited on a BaF₂ pellet in laminate (the formulation is sandwiched between two polypropylene films to avoid the re-oxygenation during the photopolymerization) or under air for irradiation with the different light sources. The evolution of the double bond content of TMPTA, the epoxy group content of EPOX, the double bond content of DVE-3, and the thiol (S-H) content of Trithiol were continuously followed by real time FTIR spectroscopy (JASCO FTIR 4100)^{39, 40} at about 1630 cm^{-1} , 790 cm^{-1} , 1620 cm^{-1} , and 2570 cm^{-1} , respectively.

TMPTA, EPOX, DVE-3, trithiol are multifunctional monomers and the conversion that is mentioned does not correspond to the monomer conversion but to the conversion of the polymerizable functions. For example, converting 50% of these functions corresponds thus already to a higher monomer conversion (order of magnitude: 75% for a difunctional monomer and 87.5% for a trifunctional one).

Photopolymerization in Water

For polymerization in water, DNND4/SBE- β -CD was combined with methyldiethanolamine (co-initiator) as a Type II photoinitiating system (DNND4/SBE- β -CD/MDEA). The monomers used, hydroxyethylacrylate (HEA) or hydroxyethylmethacrylate

(HEMA), are characterized by a good solubility in water. The monomer dissolved in water and in presence of a photoinitiating system was irradiated in a glass vial using a LED@405 nm. The polymerization was carried out under air. The water content in the prepared gel was determined by thermogravimetric analysis (TGA) (METTLER – TOLEDO TGA 851e).

Steady State Photolysis Experiments

The studied photoinitiators in the presence of an additive (*e.g.* Iod or R-Cl) in acetonitrile were irradiated with the LED at 405 nm, and the UV-vis spectra were recorded using a JASCO V-530 UV/Vis spectrophotometer at different irradiation time.

Fluorescence Experiments

The fluorescence properties of the investigated photoinitiators in acetonitrile were studied using a JASCO FP-750 Spectrofluorimeter. The interaction rate constants k_q between the studied photoinitiator and the quencher were extracted from classical Stern-Volmer plots⁴ ($I_0/I = 1 + k_q\tau_0[\text{quencher}]$, where I_0 and I stand for the fluorescence intensity of the photoinitiator in the absence and the presence of the quencher, respectively; τ_0 stands for the lifetime of the excited photoinitiator in the absence of quencher).

Redox Potentials

The oxidation potentials (E_{ox} vs SCE) of the studied photoinitiators were measured in acetonitrile by cyclic voltammetry with tetrabutylammonium hexafluorophosphate (0.1 M) as a supporting electrolyte (Voltalab 6 Radiometer). The procedure has been presented in detail in ref.⁴¹ The free energy change ΔG for an electron transfer between photoinitiators and Iod (or R-Cl) can be calculated from the classical Rehm-Weller equation: $\Delta G = E_{ox} - E_{red} - E_S$ (or E_T) + C ; where E_{ox} , E_{red} , E_S (or E_T), and C are the oxidation potential of the studied

photoinitiators, the reduction potential of Iod (or R-Cl), the excited singlet (or triplet) state energy of the studied photoinitiators, and the electrostatic interaction energy for the initially formed ion pair.⁴² This latter parameter is generally considered as negligible in polar solvents.

ESR Spin Trapping (ESR-ST) Experiment

ESR-ST experiment was carried out using an X-Band spectrometer (MS 400 Magnettech). The radicals were generated at room temperature upon the LED@405 nm exposure under N₂ and trapped by phenyl-*N-tert*-butylnitron (PBN) according to a procedure⁴³ described elsewhere in detail. The ESR spectra simulations were carried out using the WINSIM software.

Laser Flash Photolysis

Nanosecond laser flash photolysis (LFP) experiments were carried out using a Q-switched nanosecond Nd/YAG laser ($\lambda_{\text{exc}} = 355$ nm, 9 ns pulses; energy reduced down to 10 mJ) from Continuum (Minilite) and an analyzing system consisted of a ceramic xenon lamp, a monochromator, a fast photomultiplier and a transient digitizer (Luzchem LFP 212).⁴⁴

RESULTS AND DISCUSSION

1/ Light Absorption Properties of the DNNDs

The UV-Visible absorption spectra of the DNNDs in acetonitrile are shown in Figure 1. As illustrated, DNND1 and DNND2 exhibit a poor ground state absorption in the visible wavelength range ($\lambda > 400$ nm) with absorption maxima located in the UV range (*i.e.* $\lambda_{\text{max}} = 329$ nm and $\lambda_{\text{max}} = 319$ nm for DNND1 and DNND2, respectively). DNND3 presents a red-shifted absorption ($\lambda_{\text{max}} = 416$ nm) compared to DNND1, probably due to the amino

substituent as already observed in other structures (see e.g. in refs.^{32, 33}). Compared to the previously reported *N*-[2-(dimethylamino)ethyl]-1,8-naphthalimide derivatives (DMAEN1 and DMAEN2) whose maxima were located in the near UV range (*i.e.* $\lambda_{\max} = 387$ nm, and $\lambda_{\max} = 391$ nm, for DMAEN1 and DMAEN2, respectively),²⁹ the absorption maxima of DNND3, DNND4 and DNND5 are successfully shifted to longer wavelength through the present careful chemical structure design (*i.e.* $\lambda_{\max} = 416$ nm, $\epsilon_{416\text{ nm}} \sim 4530 \text{ M}^{-1}\text{cm}^{-1}$; $\lambda_{\max} = 431$ nm, $\epsilon_{431\text{ nm}} \sim 7970 \text{ M}^{-1}\text{cm}^{-1}$ and $\lambda_{\max} = 451$ nm, $\epsilon_{451\text{ nm}} \sim 17940 \text{ M}^{-1}\text{cm}^{-1}$ for DNND3; DNND4 and DNND5, respectively). The extended light absorption range of these three compounds make them adapted to a wider range of LED devices (*i.e.* from near UV to blue LED).

For the different DNNDs, a charge transfer transition (HOMO→LUMO) is found for the lowest energy transition in agreement with their good light absorption properties. Indeed, for DNND1 to DNND4, the Highest Occupied Molecular Orbital (HOMO) and Lowest Unoccupied Molecular Orbital (LUMO) are clearly localized on the amino substituent and on the naphthalimide moiety, respectively (Figure 2). For DNND5, such a charge transfer transition is also found but the HOMO and LUMO are more delocalized on the π scaffold.

Figure 1. UV-visible absorption spectra of the DNNDs in acetonitrile.

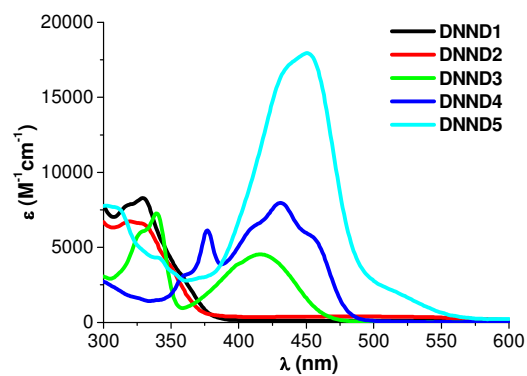
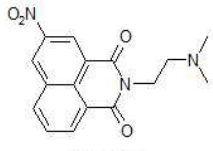
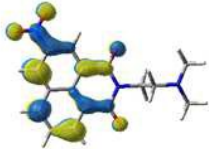
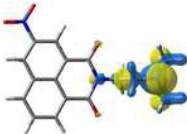
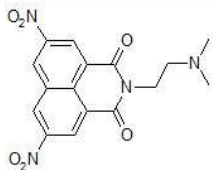
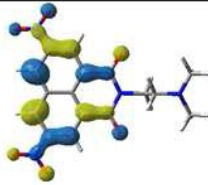
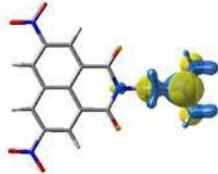
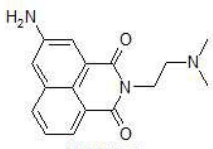
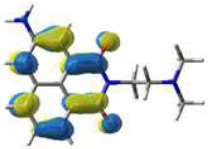
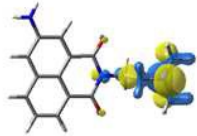
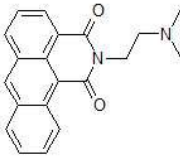
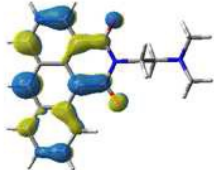
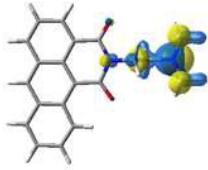
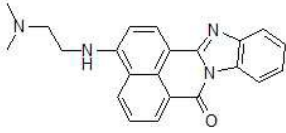
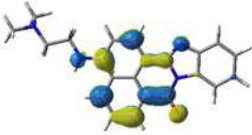


Figure 2. Highest Occupied Molecular Orbital (HOMO) and Lowest Unoccupied Molecular Orbital (LUMO) of DNNDs at UB3LYP/6-31G* level (isovalue=0.04).

	LUMO	HOMO
 DNND1		
 DNND2		
 DNND3		
 DNND4		
 DNND5		

2/ Photoinitiating Ability of the DNNDs based Photoinitiating Systems

2a/ DNNDs for the Cationic Photopolymerization of Epoxides

The DNNDs were combined with various additives (*i.e.* Iod and NVK) to initiate the ring-opening CP of EPOX under air using different irradiation devices (*i.e.* halogen lamp or LEDs centered at 365 nm, 385 nm, 405 nm, 455 nm or 470 nm). Figure 3 displays some typical conversion-time profiles for the CP of EPOX and final epoxy function conversions FC at $t = 800$ s are summarized in Table 1. DNND2 exhibited light absorption only in UV range, however, the DNND2 based systems (DNND2/Iod or DNND2/Iod/NVK) cannot initiate the

polymerization of EPOX under the LED at 365 nm due to their poor light absorption properties and the low light intensity of this LED@365 nm ($\sim 18 \text{ mW cm}^{-2}$). With the DNND1 (or DNND4)/Iod combination, no polymerization was observed under the LED at 405 nm irradiation. The addition of NVK (as in previously reported photoinitiating systems⁴⁵) significantly enhanced the *FC* (36% and 63% for DNND1 and DNND4 based systems, respectively). DNND4/Iod/NVK also worked well under the LED at 455 nm irradiation (*FC* = 57%, curve 6 in Figure 3). Remarkably, the DNND3/Iod and DNND5/Iod two-component systems already exhibited an excellent efficiency: *FC* attained 66% (curve 1 and curve 4 in Figure 3) and tack-free polyether coatings were obtained after 800 s of irradiation (LED at 405 nm) due to the excellent overlapping between their absorption spectra and the emission spectrum of the LED. Moreover, these two efficient systems resulted in relatively high monomer conversions (42% and 43%) under a halogen lamp irradiation, while the CQ based reference systems (CQ/Iod or CQ/Iod/NVK) yielded no polymerization. Interestingly, the DNND3/Iod led to EPOX conversions of 44%, 66% and 68% under LED at 385nm, 455nm and 470 nm, respectively. After one week of storage at room temperature, the photoinitiating ability of DNND3/Iod did not change (Figure S7 (a) in SI), indicating a good shelf life stability of the formulations. By analogy with the general behavior of other previously investigated photoinitiating systems^{30, 32, 33}, the generation of cations, radical cations and radicals upon light exposure of the DNND/Iod and DNND/Iod/NVK systems can be safely described by the following set of reactions (r1-r5).

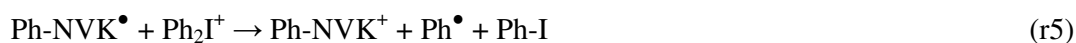
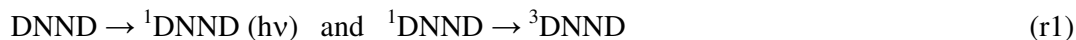


Figure 3. Photopolymerization profiles of EPOX (epoxy function conversion vs. time) under air in the presence of DNNDs based PISs: (a) DNND3/Iod upon the LED at 405 nm (curve 1), 455 nm (curve 2) or 470 nm (curve 3) exposure; DNND5/Iod upon the LED at 405 nm exposure (curve 4); DNND4/Iod/NVK upon the LED at 405 nm (curve 5) or 455 nm (curve 6) exposure; DNNDs: 0.5wt%; Iod: 2wt%; NVK: 3wt% in the formulations.

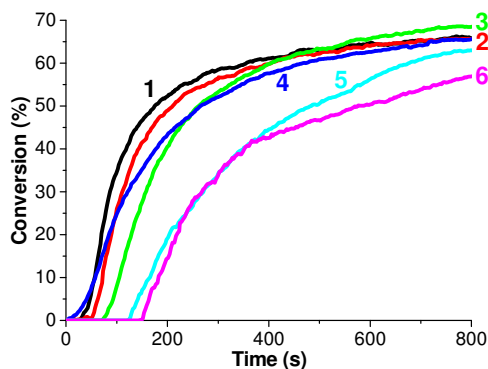


Table 1. Epoxy function conversions obtained under air upon exposure to different light sources for 800 s in the presence of DNNDs/Iod (0.5%/2%, w/w) or DNNDs/Iod/NVK (0.5%/2%/3%, w/w/w).

PIS	LED (365nm)	LED (385nm)	LED (405 nm)	LED (455 nm)	LED (470 nm)	Halogen lamp
DNND1/Iod			np ^a			
DNND2/Iod	np ^a					
DNND3/Iod		44%	66% 67% ^b	66%	68%	42%
DNND4/Iod			np ^a			
DNND5/Iod			66%			43%
DNND1/Iod/NVK		15%	36%			
DNND2/Iod/NVK	np ^a					
DNND4/Iod/NVK			63%	57%		
CQ/Iod						np ^a
CQ/Iod/NVK						np ^a

^a np: no photopolymerization;

^b measured after one week of storage at room temperature.

2b/ DNNDs in the Free Radical Photopolymerization of An Acrylate

The ability of the DNNDs based photoinitiating systems (consisting of one, two or three components) to initiate the free radical photopolymerization FRP of TMPTA in laminate or under air was also investigated. Typical conversion-time profiles for the FRP of TMPTA in laminate upon the exposure to different LEDs are shown in Figure 4 and the final acrylate

function conversions FC are listed in Table 2. As illustrated in Figure 4 (a), when using the LED at 405 nm: (i) DNND3 alone was capable of initiating the TMPTA polymerization but led to a low FC (25%); (ii) the DNND1/R-Cl, DNND2/Iod (even though it cannot work under LED@365 nm, it does under LED@405 nm due to the high light intensity of this LED) and DNND4/Iod two-component systems also led to relatively low polymerization rates and conversions ($FC = 29\% \sim 41\%$, curve 1, 2 and 7); (iii) the DNND3/R-Cl and DNND3/Iod were more efficient and yielded excellent final conversions (60% and 57%, respectively, curve 4 and 5 in Figure 4 (a)) slightly better than that reached with the popular commercial photoinitiator BAPO (56%); (iv) interestingly, a noticeable bleaching in the presence of DNND4/Iod (Table S1 in the SI) was observed after the photopolymerization which endows the system with potential applications in the manufacture of colorless coatings; (v) the addition of NVK to the DNND3/Iod or DNND4/Iod system significantly increased the polymerization efficiency, leading to final conversions of 63% and 55%, respectively (curve 5 vs curve 6, curve 7 vs curve 8 in Figure 4 (a)); (vi) a high FC (61%) was also found when using the DNND5/MDEA/R-Cl combination.

TMPTA was also polymerized under a LED@385 irradiation: DNND1/R-Cl presented a slightly better efficiency than under the LED@405, while the opposite was found with DNND3/Iod (Figure 4 (b) and Figure S8, curve 1 and curve 2). When the LED at 455 nm was used, DNND3/Iod, DNND5/R-Cl and DNND5/MDEA/R-Cl demonstrated a similar or better efficiency ($FC = 53\% \sim 64\%$, Figure 4 (b) and Figure S8, curve 3, 5 and 6) than the BAPO reference photoinitiator ($FC = 54\%$). DNND5/MDEA/R-Cl also worked well upon exposure at 470 nm and produced a $FC = 58\%$. Compared to the CQ/Iod reference system ($FC = 18\%$), DNND3/Iod and DNND5/R-Cl were more efficient, and led to higher FC ($\geq 32\%$, Figure 4 (c)) under the soft halogen lamp irradiation. DNND5/R-Cl also exhibited a better efficiency than another CQ based reference system (CQ/MDEA). A good storage stability was found

(see Figure S7 in SI) for the photocurable acrylate formulations containing various DNNDs based photoinitiating systems (*i.e.* DNND3/Iod/NVK, DNND5/R-Cl and DNND5/MDEA/R-Cl). The R-Cl and MDEA additives function on the basis of reactions (r6-r10) as already proposed in other systems.^{30, 46}



Figure 4. Photopolymerization profiles of TMPTA (acrylate function conversion vs. time) in laminate in the presence of DNNDs based PISs: (a) DNND1/R-Cl (curve 1), DNND2/Iod (curve 2), DNND3 (curve 3), DNND3/R-Cl (curve 4), DNND3/Iod (curve 5), DNND3/Iod/NVK (curve 6), DNND4/Iod (curve 7), DNND4/Iod/NVK (curve 8), DNND5/MDEA/R-Cl (curve 9) upon the exposure to LED at 405 nm; (b) DNND1/R-Cl (curve 1) or DNND3/Iod (curve 2) upon the exposure to LED at 385 nm; DNND3/Iod (curve 3), DNND4/Iod/NVK (curve 4), DNND5/R-Cl (curve 5) or DNND5/MDEA/R-Cl (curve 6) upon the exposure to LED at 455 nm; DNND5/MDEA/R-Cl upon the exposure to LED at 470 nm (curve 7); (c) DNND3/R-Cl (curve 1) or DNND5/R-Cl (curve 2) upon the exposure to halogen lamp; CQ/Iod (0.5%/2%, w/w) or CQ/MDEA (0.5%/2%, w/w) upon the halogen lamp exposure and BAPO (0.5 wt%) upon the LED at 405 nm (a) or 455 nm (b) exposure as references; DNNDs: 0.5 wt%; Iod or MDEA: 2 wt%; NVK or R-Cl: 3wt% in the formulations.

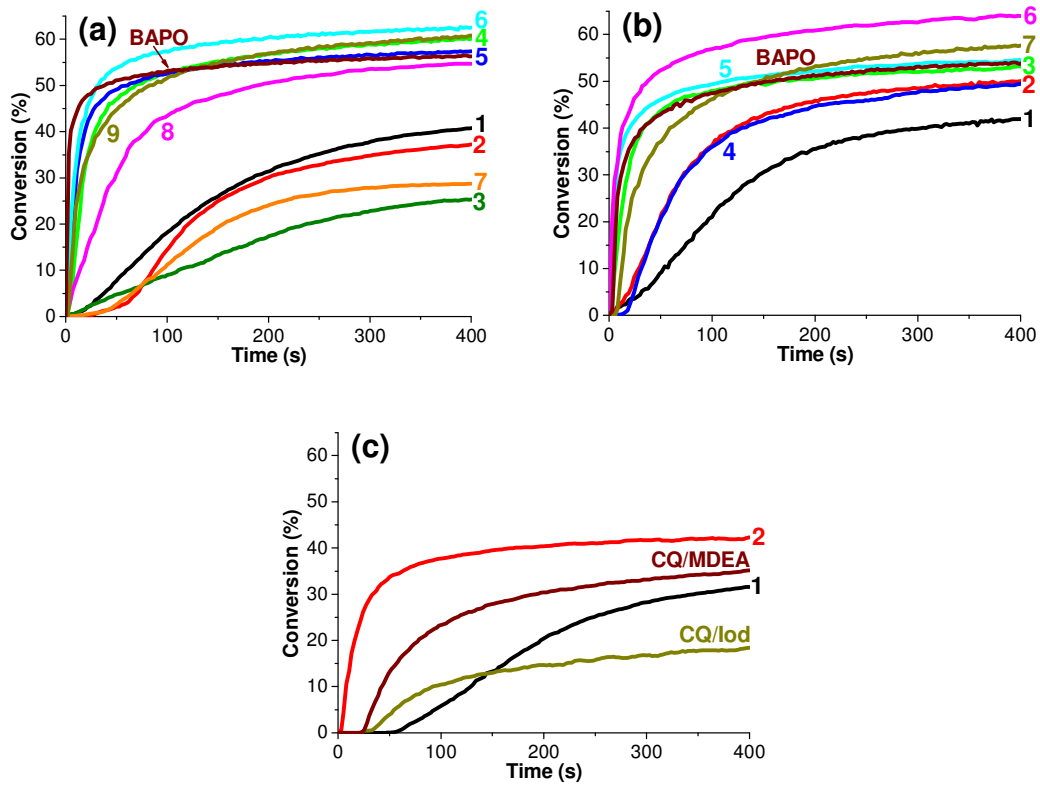


Table 2. Acrylate function conversions obtained in laminate upon exposure to different light sources for 400 s in the presence of DNNDs based PISs (DNNDs: 0.5 wt%; Iod or MDEA 2wt%; NVK or R-CI: 3 wt% in the formulations); CQ/Iod (0.5%/2%, w/w), CQ/MDEA (0.5%/2%, w/w) and BAPO (0.5 wt%) PISs as references.

PIS	LED 385 nm	LED 405 nm	LED 455nm	LED 470nm	Halogen lamp
DNND1/R-CI	42%	41%			
DNND2/Iod		37%			
DNND3		25%	np ^a		
DNND3/R-CI		60%			32%
DNND3/Iod	50%	57%	53%		
DNND3/Iod/NVK		63% 63% ^b			
DNND4/Iod		29%			
DNND4/Iod/NVK		55%	49%		
DNND5			np ^a		
DNND5/R-CI			54% 54% ^b		42%
DNND5/MDEA/R-CI		61%	64% 61% ^b	58%	
BAPO		56%	54%		
CQ/Iod					18%
CQ/MDEA					35%

^a np: no photopolymerization;

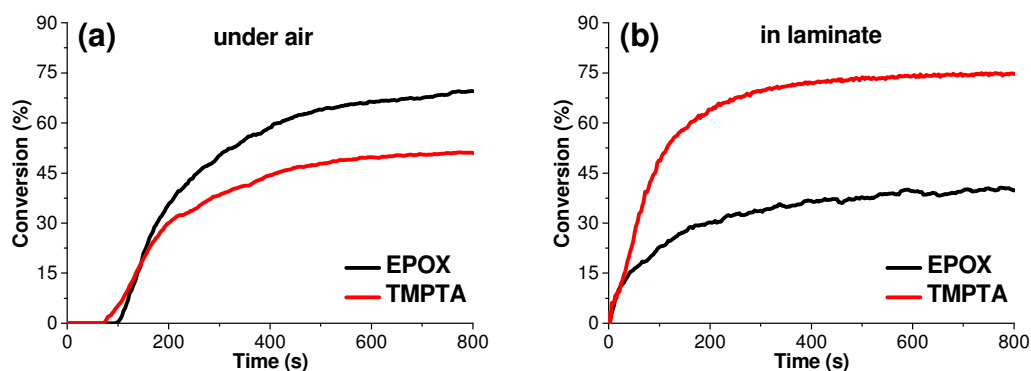
^b measured after one week of storage at room temperature.

2c/ DNNDs for the IPN Synthesis: Photopolymerization of EPOX/TMPTA

Blends

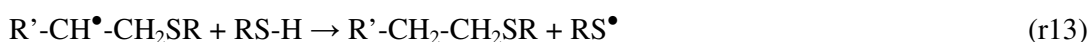
The DNND4/Iod/NVK combination was able to initiate the concomitant cationic/radical polymerization of an EPOX/TMPTA blend (50%/50% w/w) upon exposure to a LED at 405 nm (Figure 5), leading to the formation of an interpenetrating polymer network (IPN). A high efficiency was found within 800s: $FC = 70\%$ for epoxy functions and $FC = 51\%$ for acrylate functions under air; $FC = 40\%$ for epoxy and $FC = 75\%$ for acrylate in laminate. Similar to the observed behavior with other photoinitiating systems,^{35, 47} the final conversions were higher in laminate for TMPTA and under air for EPOX. Tack free coatings were obtained after 8 min of the LED irradiation either in laminate or under air and the color of the coating became lighter after the polymerization (Table S1).

Figure 5. Photopolymerization profile of an EPOX/TMPTA blend (50%/50%, w/w) in the presence of DNND4/Iod/NVK (0.5%/2%/3%, w/w/w) under air (a) or in laminate (b). LED at 405 nm exposure (conversion of epoxy (or acrylate) function vs. time)).



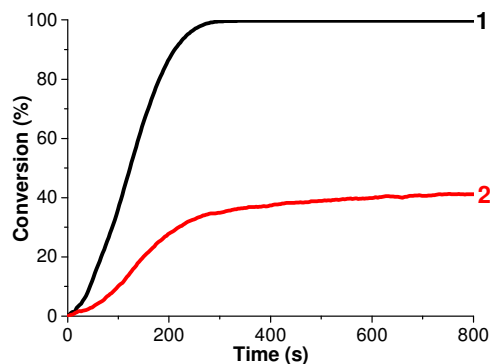
2d/ DNNDs for a Thiol–Ene Photopolymerization

The thiol–ene (trithiol/DVE-3) polymerization was also carried out using the DNND4/Iod system upon exposure to the LED at 405 nm (Figure 6). The plausible mechanism is summarized in reactions 1-3 followed by reactions 11-13.



The low S–H conversion (~41% vs ~100% for the vinyl double bond after 800 s of light exposure) indicates a significant contribution of the cationic polymerization of DVE-3.

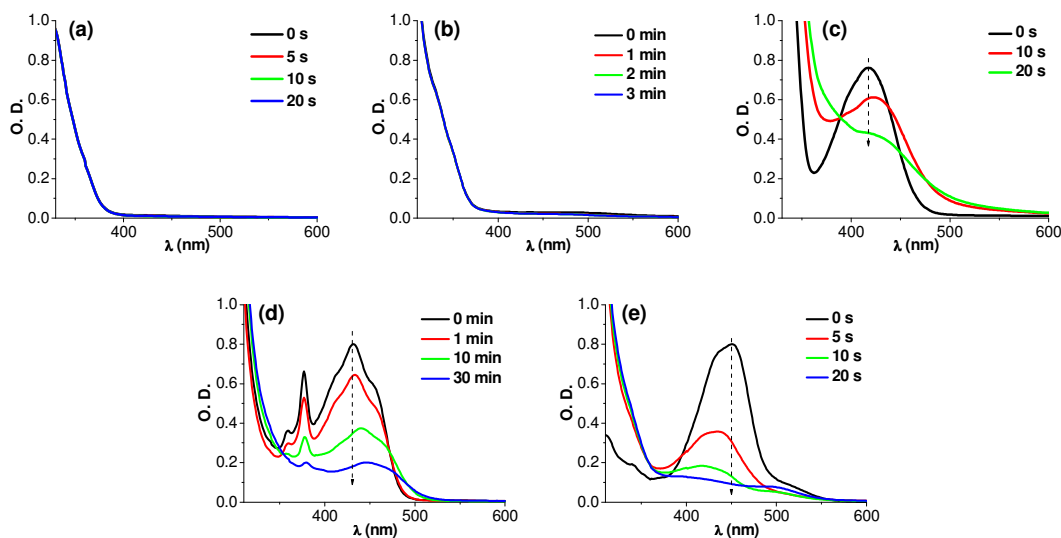
Figure 6. Photopolymerization profile of a trithiol/DVE-3 blend (40%/60%, n/n; 57%/43%, w/w) in laminate in the presence of DNND4/Iod (0.5%/2%, w/w) upon the LED at 405 nm exposure; curve 1: DVE-3 (vinyl double bond) conversion; curve 2: trithiol (S–H) conversion.



3/ Photochemistry of the DNNDs based Photoinitiating Systems

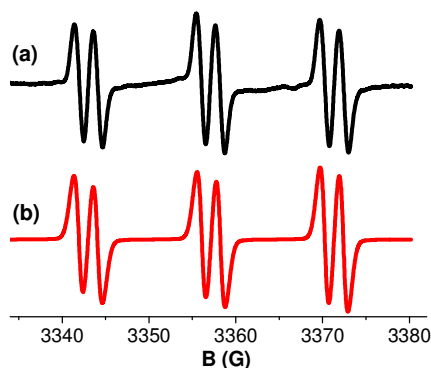
The DNND/Iod interaction was qualitatively investigated using steady state photolysis experiments in acetonitrile (Figure 7 and Figure S9). During the irradiation at 405 nm under air, a very fast bleaching of both DNND3/Iod (or R-Cl) and DNND5/Iod (or R-Cl) was observed within 20 s [Figure 7 (c) and (e), Figure S9 (b-2) and (d-2)]; for DNND4/Iod, a notable bleaching occurred, but at a moderate pace], whereas a photochemical stability of DNND1/Iod and DNND2/Iod was noted (Figure 7 (a) and (b)): this is in line with the trend observed for the corresponding polymerization efficiencies.

Figure 7. Steady state photolysis of DNNDs/Iod in acetonitrile: (a) DNND1/Iod, (b) DNND2/Iod, (c) DNND3/Iod, (d) DNND4/Iod and (e) DNND5/Iod; UV-visible spectra recorded at different irradiation time. [Iod] = 15 mM. Upon the LED at 405 nm exposure.



The behaviors of the DNNDs in multi-component systems were further investigated by ESR spin trapping experiments. Phenyl radicals were clearly observed e.g. after the electron transfer in the DNND3/Iod couple (PBN spin adduct in Figure 8; hfc: $a_N = 14.2$ G; $a_H = 2.2$ G; reference values in refs.^{48,49}), which is consistent with the mechanism described in the set of reactions r1-r3.

Figure 8. ESR spectra of the radicals generated in DNND3/Iod and trapped by PBN in *tert*-butylbenzene: (a) experimental and (b) simulated spectra.



The first excited singlet state of the DNNDs (1 DNND) was characterized from fluorescence experiments. Long fluorescence lifetimes (τ) are critical for efficient interactions

between $^1\text{DNND}$ and the additives. As illustrated in Table 3, the fluorescence quantum yields (Φ_{fluo}) largely depend on the substituents on the DNND skeleton and follow the trend: $\text{DNND2} < \text{DNND1} < \text{DNND4} < \text{DNND5} < \text{DNND3}$. The nitro derivative (DNND1), compared to the corresponding amino one (DNND3) has much lower Φ_{fluo} and τ values: DNND1 (5.2 ns) $<$ DNND3 (15.2 ns). The DNND1/Iod (or R-Cl) and DNND3/Iod (or R-Cl) interaction rate constants determined by fluorescence quenching experiments are almost diffusion-controlled: $k_q = 11.3 \times 10^9 \text{ M}^{-1}\text{s}^{-1}$ ($16.4 \times 10^9 \text{ M}^{-1}\text{s}^{-1}$) and $3.2 \times 10^9 \text{ M}^{-1}\text{s}^{-1}$ ($2 \times 10^9 \text{ M}^{-1}\text{s}^{-1}$), respectively. The free energy changes ΔG for the $^1\text{DNND1}$ ($^1\text{DNND3}$, $^1\text{DNND4}$ or $^1\text{DNND5}$)/Iod (or R-Cl) electron transfer reactions (reactions r2 and r9) are highly negative, which makes the processes favorable. This is also in full agreement with the high electron transfer quantum yields (Φ_{eT}) found for reactions 2 and 9 (Table 3). The reaction 2 and 9 being favorable for all the DNNDs, their respective light absorption properties must be taken into account to explain the difference in their photoinitiating ability.

$^1\text{DNND}$ might undergo an intersystem crossing process to yield a triplet state ($^3\text{DNND}$). However, no DNND triplet state absorption was observed in the 400-700 nm range by laser flash photolysis experiments: this was probably due to a low intersystem crossing quantum yield. Therefore, the DNNDs likely react with the additives mainly in their singlet state (a triplet route remains, however, energetically favourable: see in Table 3, $\Delta G_T < 0$).

Table 3. Parameters characterizing the reactivity of the investigated DNNDs with various additives.

	E_s (eV) ^a	E_{ox} (V vs. SCE) ^b	ΔG_s (eV) ^c	E_T (eV) _d	ΔG_T (eV) ^e	k_q ($\times 10^9 \text{ M}^{-1}\text{s}^{-1}$) ^f	Φ_{eT} ^g	Φ_{fluo} ^h	τ^1 (ns)
DNND1/Iod	2.96	0.83	-1.93	2.26	-1.23	11.3	0.73	5.6×10^{-4}	5.2
DNND1/R-Cl	2.96	0.83	-1.35	2.26	-0.65	16.4	0.85	5.6×10^{-4}	5.2
DNND2		0.72		2.18				9.8×10^{-5}	
DNND3/Iod	2.68	0.62	-1.86	2.03	-1.21	3.2	0.69	0.16	15.2
DNND3/R-Cl	2.68	0.62	-1.28	2.03	-0.63	2.0	0.68	0.16	15.2

DNND4/Iod	2.66	0.59	-1.87	1.59	-0.8	0.012	15.0
DNND4/R-Cl	2.66	0.59	-1.29	1.59	-0.22	0.012	15.0
DNND5/Iod	2.59	0.52	-1.87	1.76	-1.04	0.017	
DNND5/R-Cl	2.59	0.52	-1.29	1.76	-0.46	0.017	

^a Singlet state energies E_S extracted from the UV-vis absorption and fluorescence emission spectra of DNNDs as usually done;

^b E_{ox} values measured by cyclic voltammetry (this work);

^{c or e} ΔG_S = free energy change for the DNNDs/additive singlet state interaction; reduction potential $E_{red} = -0.2$ V for Iod¹, $E_{red} = -0.78$ V for R-Cl⁵⁰; ΔG_T = free energy change for the DNNDs/additive triplet state interaction.

^d Triplet state energies E_T calculated at UB3LYP/6-31G* level in molecular orbital calculations;

^f $k_q = {}^1$ DMAENs/additive interaction rate constant measured by fluorescence quenching experiments;

^g Φ_{eT} = DNNDs/additive electron transfer quantum yields in the singlet state calculated according to $\Phi_{eT} = k_q\tau_0 [\text{additive}]/(1 + k_q\tau_0 [\text{additive}])^1$, ([additive]: [Iod] = 4.7×10^{-2} M; [R-Cl] = 6.9×10^{-2} M in the formulations).

^h fluorescence quantum yields (Φ_{flu})

ⁱ fluorescence lifetimes (τ).

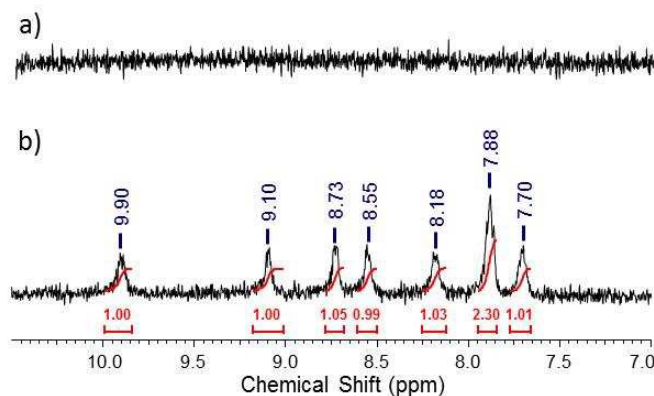
4/ Polymerization in water for the synthesis of hydrogels

4a/ Synthesis and characterization of the water soluble DNND/SBE- β -CD

complex

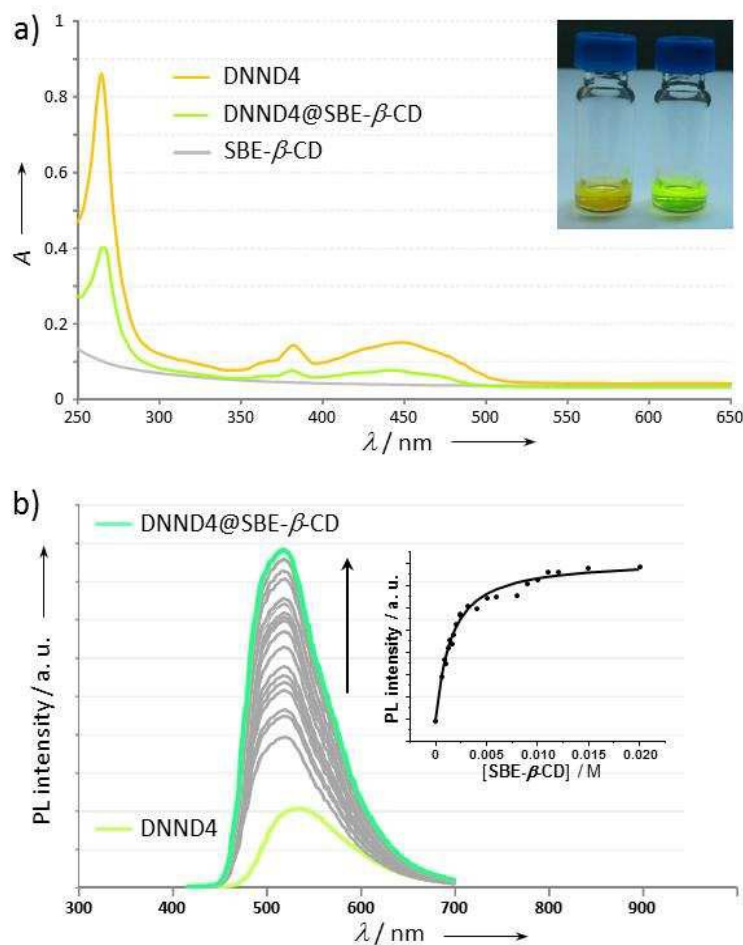
After having prepared the DNNDs derivatives and characterized their photoreactivity, we looked toward an inclusion complexation strategy⁵¹⁻⁵⁴ that would enable to increase the water solubility of the PI enough to allow the photopolymerization reactions in water. After several unsuccessful trials, we managed to prepare an azonafide (DNND4) complex with sulfobutylether- β -cyclodextrin (SBE- β -CD, see SI).⁵⁵ This modified β -cyclodextrin has several sulfobutylether moieties as a mean to enhance both the solubility of the macrocyclic host and slightly extend the cavity size. This compound was found to greatly enhance the solubility of some drugs in pharmacological studies. ¹H NMR spectroscopy of DNND4 in water showed virtually no signals (Figure 9).

Figure 9. a) 400 MHz ¹H NMR spectra of DNND4 alone (1 mM) and b) that of the complex (~20 mM) in D₂O.



However, the complex showed resonances in the aromatic region assigned to include DNND4 within the cavity of SBE- β -CD. The ratio of integrals between guest aromatic protons and those of SBE- β -CD is about 1/24 reflecting a rather low but sufficient complexation capacity. The complexation can be seen visually since the brownish opaque suspension of DNND4 turned yellowish transparent after complexation (Figure 10a, inset).

Figure 10. a) UV-vis spectra of DNND4 (0.1 mM), SBE- β -CD (0.1 mM) and of the complex (0.1 mM based on the molecular weight of SBE- β -CD since the guest is highly diluted). b) Fluorescence titration of DNND4 (5×10^{-4} M) with increasing concentration of SBE- β -CD (from 6×10^{-4} M to 20 mM. $\lambda_{\text{exc}} = 382$ nm).



The fluorescence of DNND4 was found to be highly sensitive to the presence of SBE- β -CD in water and then fluorescence titrations were performed to estimate the binding constant (Figure 10b). Considering that the observed fluorescence is a weighted contribution of that of free DNND4 and that of complexed DNND4 and using an adapted version for a 1:1 binding model (equation 1),^{56, 57} the set of experimental points (intensity measured at 519 nm) was fitted to this equation using a non linear curve fit and provided a binding constant $K_a = 796 \pm 60 \text{ M}^{-1}$ (Figure 10b inset) which is consistent with expected values.^{58, 59}

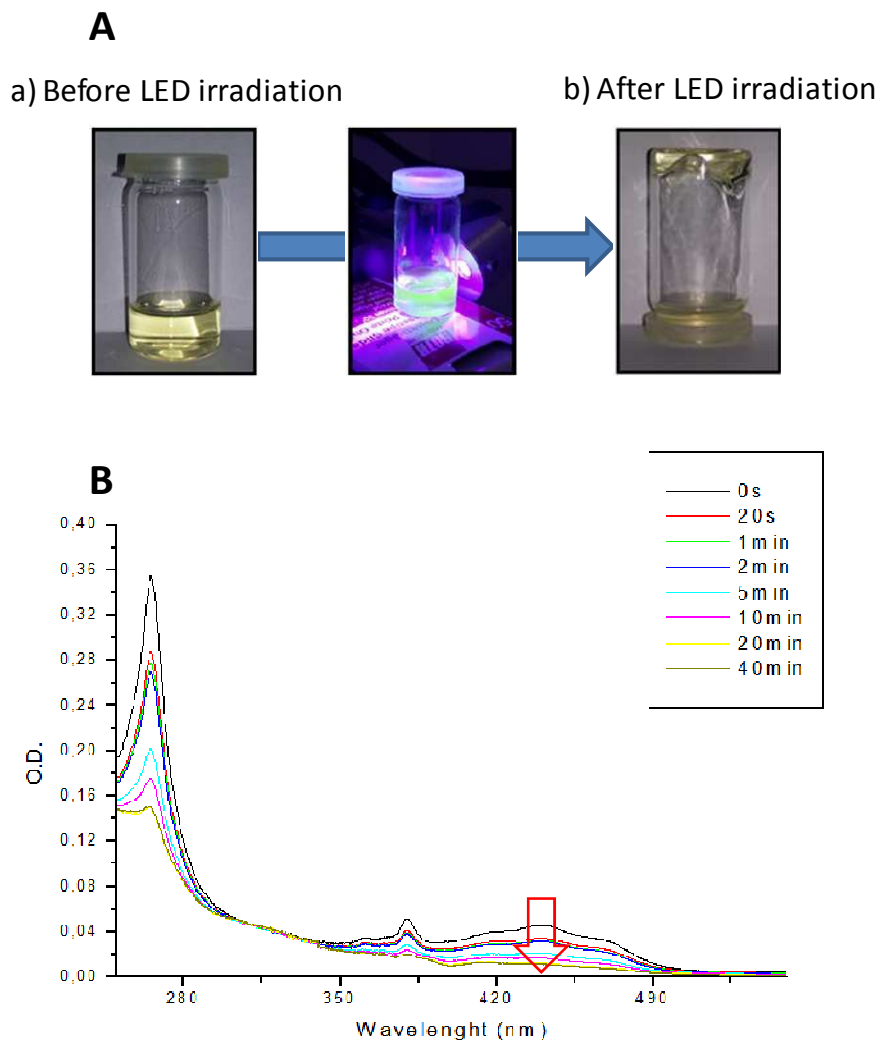
$$F_x = F_0 - \left(\frac{\Delta F}{2} \right) \left[\left(1 + \frac{[H]_0}{[G]_0} + \frac{1}{K[G]_0} \right) - \sqrt{\left(1 + \frac{[H]_0}{[G]_0} + \frac{1}{K[G]_0} \right)^2 - 4 \frac{[H]_0}{[G]_0}} \right] \quad (\text{Eq. 1})$$

The present results indicate that the hydrophobic DNND4 is included in the cavity of SBE- β -CD which is reflected by the observable ^1H NMR resonances of the guest in the complex in water and the changes in UV and Fluorescence spectra.

4b/ DNND4/SBE- β -CD/MDEA as water soluble photoinitiating system

A Type II photoinitiating system [DNND4/SBE- β -CD (0.3%)/MDEA (4%)] was used for the photopolymerization of HEMA in water ($[\text{HEMA}] = 1.5 \text{ M}$ in water). After 1h of LED@405 nm (110 mW/cm²), the formation of a gel is clearly observed (Figure 11A). Remarkably, it was not necessary to use inert atmosphere showing the high reactivity of the photoinitiating system to overcome the oxygen inhibition. The monomer conversion was determined gravimetrically (~68%) and the water content (~70%) for the synthesized hydrogels determined by thermogravimetric measurement. Without MDEA or DNND4/SBE- β -CD, no polymerization occurs showing that both components are crucial for an efficient photoinitiating system in agreement with the reaction r7. In full agreement with r7, a clear bleaching is observed for the photolysis of a DNND4/SBE- β -CD/MDEA solution in water (Figure 11B). The photopolymerization of hydroxyethylacrylate (HEA) was also easily accessible upon the same conditions than HEMA.

Figure 11. (A) Description of the polymerization in water upon LED@405 nm irradiation; (B) photolysis of a DNND4/SBE- β -CD/MDEA solution in water upon LED@405 nm irradiation.



CONCLUSION:

By changing the substituents on the *N*-[2-(dimethylamino)ethyl]-1,8-naphthalimide skeleton, the light absorption maxima were successfully shifted to the visible range. Upon exposure of the DNNDs in the presence of an iodonium salt (Iod), *N*-vinylcarbazole (NVK), an amine (MDEA or EDB) or 2,4,6-*tris*(trichloromethyl)-1,3,5-triazine (R-Cl) to various visible LED lights (centered at 405 nm, 455 nm and 470 nm), radicals, cation radicals and cations were photochemically generated. The cationic polymerization of EPOX, the free radical

polymerization of TMPTA, the EPOX/TMPTA blend IPN polymerization, the trithiol/DVE-3 thiol-ene polymerization were achieved. Some of these DNND based photoinitiating systems (*e.g.* DNND3/Iod, DNND3/R-Cl) are more efficient than the well-known CQ based reference systems or BAPO. The synthesis of hydrogels was also feasible using a DNND derivative encapsulated in a cyclodextrin. This research extends the range of high-performance photoinitiating systems operating under violet to blue lights. Other works are in progress.

ASSOCIATED CONTENT

Supporting Information

Syntheses of DNNDs; emission spectra of the different irradiation devices; storage stability of the studied PISs in the formulations; Steady state photolysis of DNNDs alone or DNNDs/additive in acetonitrile; Color change of TMPTA or EPOX/TMPTA (50%/50%, w/w) film after photopolymerization. This information is available free of charge via the Internet.

Corresponding Author

*E-mail: jacques.lalevee@uha.fr (J.L.)

pu.xiao@uha.fr (P.X.)

Notes

The authors declare no competing financial interest.

ACKNOWLEDGMENTS:

JL thanks the Institut Universitaire de France for the financial support.

REFERENCES:

1. J. P. Fouassier and J. Lalevée, *Photoinitiators for Polymer Synthesis-Scope, Reactivity, and Efficiency*, Weinheim: Wiley-VCH Verlag GmbH & Co KGaA, , 2012.
2. N. S. Allen, *Photochemistry and photophysics of polymer materials*, Wiley, USA, 2010.
3. J. V. Crivello and K. Dietliker, *Photoinitiators for Free Radical, Cationic and Anionic Photopolymerization, 2nd edition*, Chichester: John Wiley & Sons, 1998.
4. J. P. Fouassier, *Photoinitiator, Photopolymerization and Photocuring: Fundamentals and Applications*, New York/Munich/Vienna: Hanser Publishers, 1995.
5. D. C. Neckers and W. Jager, *Photoinitiation for Polymerization: UV and EB at the Millenium*, John Wiley & Sons, Chichester, 1999. 410 pp.
6. D. Neshchadin, A. Rosspeintner, M. Griesser, B. Lang, S. Mosquera-Vazquez, E. Vauthey, V. Gorelik, R. Liska, C. Hametner, B. Ganster, R. Saf, N. Moszner and G. Gescheidt, *J. Am. Chem. Soc.*, 2013, **135**, 17314-17321.
7. F. Sun, Y. Li, N. Zhang and J. Nie, *Polymer*, 2014, **55**, 3656-3665.
8. K. Kawamura, C. Ley, J. Schmitt, M. Barnet and X. Allonas, *J. Polym. Sci., Part A : Polym. Chem.*, 2013, **51**, 4325-4330.
9. H. Kitano, K. Ramachandran, N. B. Bowden and A. B. Scranton, *J. Appl. Polym. Sci.*, 2013, **128**, 611-618.
10. W. D. Cook and F. Chen, *Polym. Chem.*, 2015, **6**, 1325-1338.
11. J. Kabatc, K. Jurek, Z. Czech and A. Kowalczyk, *Dyes Pigm.*, 2015, **114**, 144-145.
12. D. Karaca Balta, Ö. Karahan, D. Avci and N. Arsu, *Prog. Org. Coat.*, 2015, **78**, 200-207.
13. G. Müller, M. Zalibera, G. Gescheidt, A. Rosenthal, G. Santiso-Quinones, K. Dietliker and H. Grützmacher, *Macromol. Rapid Commun.*, 2015, **36**, 553-557.
14. A. Aguirre-Soto, C.-H. Lim, A. T. Hwang, C. B. Musgrave and J. W. Stansbury, *J. Am. Chem. Soc.*, 2014, **136**, 7418-7427.
15. J. E. Klee, M. Maier and C. P. Fik, in *Dyes and Chromophores in Polymer Science*, eds. J. Lalevée and J.-P. Fouassier, John Wiley & Sons, Inc., 2015, pp. 123-138.
16. R. Bongiovanni and M. Sangermano, in *Encyclopedia of Polymer Science and Technology*, John Wiley & Sons, Inc., 2002.
17. B. Strehmel, T. Brömme, C. Schmitz, K. Reiner, S. Ernst and D. Keil, in *Dyes and Chromophores in Polymer Science*, eds. J. Lalevée and J.-P. Fouassier, John Wiley & Sons, Inc., 2015, pp. 213-249.
18. C. I. Vallo and S. V. Asmussen, in *Photocured Materials*, eds. A. Tiwari and A. Polykarpov, The Royal Society of Chemistry, 2015, pp. 321-346.
19. J. Crivello, in *Dyes and Chromophores in Polymer Science*, eds. J. Lalevée and J.-P. Fouassier, John Wiley & Sons, Inc., 2015, pp. 45-79.
20. S. Doran, O. S. Taskin, M. A. Tasdelen and Y. Yağci, in *Dyes and Chromophores in Polymer Science*, eds. J. Lalevée and J.-P. Fouassier, John Wiley & Sons, Inc., 2015, pp. 81-121.
21. J. Torgersen, X.-H. Qin, Z. Li, A. Ovsianikov, R. Liska and J. Stampfl, *Advanced Functional Materials*, 2013, **23**, 4542-4554.
22. T. Gong, B. J. Adzima, N. H. Baker and C. N. Bowman, *Adv. Mater.*, 2013, **25**, 2024-2028.
23. B. P. Fors and C. J. Hawker, *Angew. Chem. Int. Ed.*, 2012, **51**, 8850-8853.

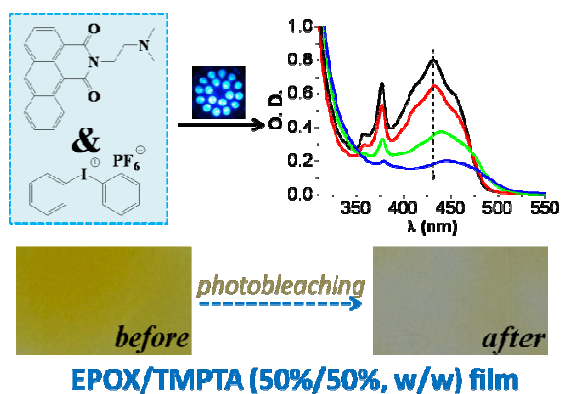
24. N. J. Treat, B. P. Fors, J. W. Kramer, M. Christianson, C.-Y. Chiu, J. R. d. Alaniz and C. J. Hawker, *ACS Macro Lett.*, 2014, **3**, 580-584.
25. T. G. Ribelli, D. Konkolewicz, S. Bernhard and K. Matyjaszewski, *J. Am. Chem. Soc.*, 2014, **136**, 13303-13312.
26. N. Karaca, G. Temel, D. Karaca Balta, M. Aydin and N. Arsu, *J. Photochem. Photobio. A: Chem.*, 2010, **209**, 1-6.
27. C. R. Rivarola, M. A. Biasutti and C. A. Barbero, *Polymer*, 2009, **50**, 3145-3152.
28. J. Lalevee and J. P. Fouassier, *Dyes and Chromophores in Polymer Science*, ISTE Wiley, London, 2015.
29. J. Zhang, N. Zivic, F. Dumur, P. Xiao, B. Graff, J. P. Fouassier, D. Gigmes and J. Lalevée, *Polymer*, 2014, **55**, 6641-6648.
30. J. Zhang, N. Zivic, F. Dumur, P. Xiao, B. Graff, D. Gigmes, J. P. Fouassier and J. Lalevée, *J. Polym. Sci., Part A: Polym. Chem.*, 2015, **53**, 445-451.
31. P. Xiao, F. Dumur, J. Zhang, B. Graff, D. Gigmes, J. P. Fouassier and J. Lalevée, *Macromol. Chem. Phys.*, 2015, **216**, 1782-1790.
32. P. Xiao, F. Dumur, J. Zhang, B. Graff, D. Gigmes, J. P. Fouassier and J. Lalevée, *J. Polym. Sci., Part A: Polym. Chem.*, 2015, **53**, 665-674.
33. P. Xiao, F. Dumur, J. Zhang, B. Graff, D. Gigmes, J. P. Fouassier and J. Lalevee, *Polym. Chem.*, 2015, **6**, 1171-1179.
34. P. Xiao, F. Dumur, B. Graff, J. Zhang, F. Morlet-Savary, D. Gigmes, J. P. Fouassier and J. Lalevée, *J. Polym. Sci., Part A: Polym. Chem.*, 2014, **53**, 567-575.
35. P. Xiao, F. Dumur, B. Graff, D. Gigmes, J. P. Fouassier and J. Lalevée, *Macromolecules*, 2014, **47**, 601-608.
36. S. M. Sami, R. T. Dorr, D. S. Alberts, A. M. Sólyom and W. A. Remers, *J. Med. Chem.*, 2000, **43**, 3067-3073.
37. J. B. Foresman and A. Frisch, *Exploring Chemistry with Electronic Structure Methods*, Gaussian. Inc., 1996.
38. M. J. Frisch, G. W. Trucks, H. B. Schlegel, G. E. Scuseria, M. A. Robb, J. R. Cheeseman, V. G. Zakrzewski, J. A. Montgomery, J. R. E. Stratmann, J. C. Burant, S. Dapprich, J. M. Millam, A. D. Daniels, K. N. Kudin, M. C. Strain, O. Farkas, J. Tomasi, V. Barone, M. Cossi, R. Cammi, B. Mennucci, C. Pomelli, C. Adamo, S. Clifford, J. Ochterski, G. A. Petersson, P. Y. Ayala, Q. Cui, K. Morokuma, P. Salvador, J. J. Dannenberg, D. K. Malick, A. D. Rabuck, K. Raghavachari, J. B. Foresman, J. Cioslowski, J. V. Ortiz, A. G. Baboul, B. B. Stefanov, G. Liu, A. Liashenko, P. Piskorz, I. Komaromi, R. Gomperts, R. L. Martin, D. J. Fox, T. Keith, M. A. Al-Laham, C. Y. Peng, A. Nanayakkara, M. Challacombe, P. M. W. Gill, B. Johnson, W. Chen, M. W. Wong, J. L. Andres, C. Gonzalez, M. Head-Gordon, E. S. Replogle and J. A. Pople, *Gaussian 03, Revision B-2*, Gaussian, Inc., Pittsburgh PA, 2003.
39. M.-A. Tehfe, J. Lalevée, S. Telitel, J. Sun, J. Zhao, B. Graff, F. Morlet-Savary and J.-P. Fouassier, *Polymer*, 2012, **53**, 2803-2808.
40. M. A. Tehfe, J. Lalevée, F. Morlet-Savary, B. Graff, N. Blanchard and J. P. Fouassier, *Macromolecules*, 2012, **45**, 1746-1752.
41. S. Erdur, G. Yilmaz, D. Goen Colak, I. Cianga and Y. Yagci, *Macromolecules*, 2014, **47**, 7296-7302.
42. D. Rehm and A. Weller, *Isr. J. Chem.*, 1970, **8**, 259-271.
43. P. Xiao, J. Lalevée, X. Allonas, J. P. Fouassier, C. Ley, M. El Roz, S. Q. Shi and J. Nie, *J. Polym. Sci., Part A: Polym. Chem.*, 2010, **48**, 5758-5766.
44. J. Lalevée, N. Blanchard, M. A. Tehfe, M. Peter, F. Morlet-Savary, D. Gigmes and J. P. Fouassier, *Polym. Chem.*, 2011, **2**, 1986-1991.

45. J. Lalevée, M.-A. Tehfe, A. Zein-Fakih, B. Ball, S. Telitel, F. Morlet-Savary, B. Graff and J. P. Fouassier, *ACS Macro Lett.*, 2012, **1**, 802-806.
46. P. Xiao, J. Zhang, F. Dumur, M. A. Tehfe, F. Morlet-Savary, B. Graff, D. Gigmes, J. P. Fouassier and J. Lalevée, *Prog. Polym. Sci.*, 2015, **41**, 32-66.
47. P. Xiao, F. Dumur, B. Graff, F. Morlet-Savary, D. Gigmes, J. P. Fouassier and J. Lalevée, *Macromolecules*, 2014, **47**, 973-978.
48. M. A. Tehfe, J. Lalevée, S. Telitel, E. Contal, F. Dumur, D. Gigmes, D. Bertin, M. Nechab, B. Graff, F. Morlet-Savary and J. P. Fouassier, *Macromolecules*, 2012, **45**, 4454-4460.
49. J. Lalevée, N. Blanchard, M. A. Tehfe, F. Morlet-Savary and J. P. Fouassier, *Macromolecules*, 2010, **43**, 10191-10195.
50. G. Wallraff, M. Baier, A. Diaz and R. Miller, *J. Inorg. Organomet. Polym.*, 1992, **2**, 87-102.
51. J. Szejtli, *Chem. Rev.*, 1998, **98**, 1743-1754.
52. J. Lagona, P. Mukhopadhyay, S. Chakrabarti and L. Isaacs, *Angew. Chem. Int. Ed.*, 2005, **44**, 4844-4870.
53. D. Bardelang, G. Casano, F. Poulhès, H. Karoui, J. Filippini, A. Rockenbauer, R. Rosas, V. Monnier, D. Siri, A. Gaudel-Siri, O. Ouari and P. Tordo, *J. Am. Chem. Soc.*, 2014, **136**, 17570-17577.
54. D. Bardelang, A. Rockenbauer, H. Karoui, J.-P. Finet, I. Biskupska, K. Banaszak and P. Tordo, *Org. Biomol. Chem.*, 2006, **4**, 2874-2882.
55. V. J. Stella and Q. He, *Toxicol Pathol.*, 2008, **36**, 30-42.
56. D. Bardelang, J.-L. Clément, J.-P. Finet, H. Karoui and P. Tordo, *J. Phys. Chem. B*, 2004, **108**, 8054-8061.
57. R. S. Macomber, *J. Chem. Educ.*, 1992, **69**, 375.
58. G. Zhang, S. Shuang, Z. Dong, C. Dong and J. Pan, *Anal. Chim. Acta*, 2002, **474**, 189-195.
59. S. Shityakov, I. Puskás, K. Pápai, E. Salvador, N. Roewer, C. Förster and J.-A. Broscheit, *Molecules*, 2015, **20**, 10264-10269.

For TOC use only:

Novel Naphthalimide-amine Based Photoinitiators Operating under Violet and Blue LEDs and Usable for Various Polymerization Reactions and Synthesis of Hydrogels.

Nicolas Zivic,^b Jing Zhang,^a David Bardelang,^b Frédéric Dumur,^b Pu Xiao,^{*,a} Thomas Jet,^{a,c} Davy-Louis Versace,^c Céline Dietlin,^a Fabrice Morlet-Savary,^a Bernadette Graff,^a Jean Pierre Fouassier,² Didier Gimes,^b and Jacques Lalevée^{*,a}



² Formerly, ENSCMu-UHA, 3 rue Alfred Werner, 68093 Mulhouse Cedex, Fr